Preprints.org

Article

Not peer-reviewed version

Microfluidic Microcirculation Mimetic for Exploring Biophysical Mechanisms of Chemotherapy-Induced Metastasis

Ashley Abraham , Sukhman Virdi , Nick Herrero , Israel Bryant , Chisom Nwakama , Megha Jacob , Gargee Khaparde , Destiny Jordan , Mackenzie McCuddin , Spencer McKinley , Adam Taylor , Conner Peeples , Andrew Ekpenyong *

Posted Date: 4 July 2023

doi: 10.20944/preprints202307.0171.v1

Keywords: microfluidics; metastasis; cancer; mechanical properties; physics of cancer; chemotherapy; microcirculation; tumor microenvironment

Preprints.org is a free multidiscipline platform providing preprint service that is dedicated to making early versions of research outputs permanently available and citable. Preprints posted at Preprints.org appear in Web of Science, Crossref, Google Scholar, Scilit, Europe PMC.

Copyright: This is an open access article distributed under the Creative Commons Attribution License which permits unrestricted use, distribution, and reproduction in any medium, provided the original work is properly cited.

Preprints (www.preprints.org) | NOT PEER-REVIEWED | Posted: 4 July 2023 doi:10.20944/preprints202307.0171.v1

Disclaimer/Publisher's Note: The statements, opinions, and data contained in all publications are solely those of the individual author(s) and contributor(s) and not of MDPI and/or the editor(s). MDPI and/or the editor(s) disclaim responsibility for any injury to people or property resulting from any ideas, methods, instructions, or products referred to in the content.

Article

Microfluidic Microcirculation Mimetic for Exploring Biophysical Mechanisms of Chemotherapy-Induced Metastasis

Ashley Abraham[1], Sukhman Virdi[2], Nick Herrero[1], Israel Bryant[2], Chisom Nwakama[3], Megha Jacob[1], Gargee Khaparde[1], Destiny Jordan[1], Mackenzie McCuddin[1], Spencer McKinley[1], Adam Taylor[1], Conner Peeples[2], and Andrew Ekpenyong[2,*]

[1] Biology Dept, Creighton University, Omaha, NE 68178; ashleyabraham@creighton.edu (AA); nickherrero@creighton.edu (NH), meghajacob@creighton.edu (MJ), gargeekhaparde@creighton.edu (GK), destinyjordan@creighton.edu (DJ), mackenziemccuddin@creighton.edu (MM), spencermckinley@creighton.edu (SM), adamtaylor@creighton.edu (AT).

[2] Physics Dept, Creighton University, Omaha, NE 68178; sukhmanvirdi@creighton.edu (SV), israelbryant@creighton.edu (IB), connerpeeples@creighton.edu (CP), andrewekpenyong@creighton.edu (AE).

[3] Chemistry Dept, Creighton University, Omaha, NE 68178; chisommwakama@creighton.edu (CN).

* Correspondence: andrewekpenyong@creighton.edu; Tel.: 1-402-280-2208

Abstract: There is rapidly emerging evidence from pre-clinical studies, patient samples and patient subpopulations that certain chemotherapeutics inadvertently produce prometastatic effects. Prior to this, we showed that doxorubicin and daunorubicin, stiffen cells before causing cell death, predisposing the cells to clogging and extravasation, the latter being a step in metastasis. Here, we investigate which other anti-cancer drugs might have similar prometastatic effects by altering the biophysical properties of cells. We treat myelogenous (K562) leukemic cancer cells with the drugs nocodazole and hydroxyurea, and then measure their mechanical properties using the microfluidic microcirculation mimetic (MMM) device, which mimics aspects of blood circulation and enables the measurement of cell mechanical properties via transit times through the device. We also quantify the morphological properties of cells to explore biophysical mechanisms underlying the MMM results. Results from MMM measurements show that nocodazole- and hydroxyurea-treated K562 cells exhibit significantly altered transit times. Nocodazole caused significant ($p < 0.01$) increase in transit times, implying a stiffening of cells. This work shows the feasibility of using the MMM to explore possible biophysical mechanisms that might contribute to chemotherapy-induced metastasis. Our work also suggests cell mechanics as a therapeutic target for much needed antimetastatic strategies in general.

Keywords: microfluidics; metastasis; cancer; mechanical properties; physics of cancer; chemotherapy; microcirculation; tumor microenvironment

1. Introduction

Although most anti-cancer drugs target the proliferation of cancer cells, it is metastasis, the complex process by which cancer cells spread from the primary tumor to other tissues and organs of the body where they form new tumors, that leads to over 90% of cancer-related deaths[1–4]. Thus, there is an urgent need for anti-metastasis therapy alongside chemotherapy and radiotherapy[5–8]. An important step in the metastatic cascade is migration[9,10] which is connected with other crucial steps as extravasation and intravasation. To migrate, cells actively alter their mechanical properties through their actin-myosin cytoskeleton[11]. We have recently shown *in vitro*[12] and others have shown in patient samples[5,7,13] that certain chemotherapeutic drugs inadvertently produce pro-metastatic effects. Interestingly, following our work, several research groups reported that certain chemotherapeutics elicit a *de novo* prometastatic tumor microenvironment in both preclinical studies and in some patient subpopulations[14–19]. Expectedly, the very notion of chemotherapy-induced metastasis was initially disconcerting since chemotherapy is one of the main pillars of cancer

© 2023 by the author(s). Distributed under a Creative Commons CC BY license.

Preprints (www.preprints.org) | NOT PEER-REVIEWED | Posted: 4 July 2023 doi:10.20944/preprints202307.0171.v1

treatment, but the aforementioned overwhelming evidence as well as newer clinical case reports[20] have not only led to a concerted search for the causal mechanisms but also to new therapeutic strategies aimed at mitigating chemotherapy-induced metastasis[21–25]. Some of the mechanisms of chemotherapy-induced metastasis reported include increase in extravasation and intravasation[15], increase in intravasation sites called tumor microenvironments of metastasis (TMEM)[16], increased migration and release of circulating tumor cells into the blood stream of cancer patients following chemotherapy[17], increased infiltration of immune cells such as neutrophils[18] and release of prometastatic proteins through extracellular vesicles[19]. Since most of these reported mechanisms involve migration, extravasation, intravasation and translocation, all of which are orchestrated by the mechanical properties of cells, a crucial question immediately presents itself: what is the role of cell mechanics in chemotherapy-induced metastasis? In other words, can cell mechanical properties orchestrate biophysical mechanisms of chemotherapy-induced metastasis?

In view of addressing this question, this work aims at showing the feasibility of using MMM to investigate which chemotherapeutic drugs alter the mechanical properties of cancer cells in ways that might inadvertently promote metastasis before cell death. This investigation is at the heart of the physics of cancer, a new research frontier which explores the mechanical properties of cancer cells and their role in cancer disease and metastasis[10,26]. Fortunately, the role of cell mechanical properties in cancer metastasis in general has also become a focus of intensive research[27,28] giving further significance to our investigation. The question that we address here, namely, whether common anti-cancer drugs inadvertently change the cytoskeleton (mechanical makeup) of various cancer cells, thereby altering cell migration, extravasation and intravasation, posits the possibility of having cell mechanical properties as therapeutic targets in the context of the ongoing search for effective anti-metastasis drugs/protocols. Interestingly, our results show that chemotherapy-induced changes to the mechanical properties of leukemic cancer cells are drug-dependent. Nocodazole, an antineoplastic agent which arrests cells in G2 or M phase and alters dynamic instability in microtubules[29], consistently induced a significant increase ($p < 0.01$) in transit times of K562 cells through the MMM, indicating increased stiffness. Hydroxyurea leads to significantly ($p < 0.0001$) reduced transit times. These results suggest new therapeutic strategies to mitigate metastases that might be induced by these drugs in the case of cancers that rely on their use. Moreover, in spite of the very wide variety of cancers with respect to their molecular biology, pathogenesis and prognosis, metastasis occurs in all cancers[4,30,31]. Thus, any contribution to anti-metastatic treatment strategies would be significant in the perennial and global fight against cancer.

Furthermore, using our simple but robust microfluidic and non-invasive tool to explore changes induced by chemotherapeutic drugs to the mechanical properties of a variety of cancer cells adds to the mechanomic library for other basic research and clinical investigations. Such a mechanomic library is useful beyond cancer research as already being envisaged in the intensely growing field of mechanical phenotyping for normal cell characterization and diseases diagnosis[32–34]. Succinctly, our work engenders innovations in three ways: novel mechanical characterization of various drug-treated cells to reveal impact of chemotherapy on cellular cytoskeleton; use of an inexpensive and yet robust microfluidic tool to discover connections between cellular mechanical properties and cancer metastasis; and provision of scientific rationale for using cell biophysical characteristics as new therapeutic targets for more effective cancer treatment.

2. Materials and Methods

2.1. Microfluidics Microcirculation Mimetic, MMM

The MMM was developed as a microfluidic tool that mimics *in vivo* pulmonary microcirculation and has been extensively used for mechanophenotyping[12,35–38]. The device mimics advection of cells in capillaries, many of which have constrictions smaller than blood cell diameters. This is also part of the circulatory phase of cancer metastasis. The MMM was developed in four main steps: (1) conceptualization/drawing using AutoCAD, (2) printing of photomask, (3) photolithography to produce master molds and (4) soft lithography for replica molding. Three variants of the MMM were

Preprints (www.preprints.org) | NOT PEER-REVIEWED | Posted: 4 July 2023 doi:10.20944/preprints202307.0171.v1

made at the AutoCAD design phase: one without constrictions (constant width of 15 μm) and the others with 5 μm and 7 μm as the smallest constriction widths. All variants have a constant height of 15 μm. A polyester photomask of the design was printed commercially (Photo Data and J.D. Photo-Tools, JD Photo Data, Hitchin, UK). Using the photomask, the master molds were fabricated following standard photolithographic techniques (Institute of Semiconductors and Microsystems, Technische Universität Dresden, Germany). An upgraded design leading to 14 devices on a single master plate has been developed (Potomac Photonics, Halethorpe, MD, USA). These master molds are used hundreds of times to make the MMM chips when needed, using soft lithography. The MMM has been used to measure the mechanical properties of resting versus activated neutrophils in the context of chronic occlusive pulmonary disorder, COPD[35,39] with results corroborating those from a different device for mechanical phenotyping, namely, the optical stretcher[40,41]. The uniqueness of MMM compared to other microfluidic devices used for mechanophenotyping is highlighted in the description below.

The MMM is made using polydimethylsiloxane (PDMS). It consists of serpentine microchannels (Figure 1) that mimic the pulmonary microcirculation, with gently tapered inlet and outlet channels (see previous publications[12,35,37,38] for 3D schematics, in addition to the pictures in Figure 1). The MMM differs from existing devices that model blood vessels in the lungs in that it does not involve branches or channel networks[42]. Rather, a single channel with constrictions in series is maintained for two reasons, namely, keeping the "view-point" of the cell and having each cell go through a large number of tractable constrictions. Firstly, from the "viewpoint" of the cell, constrictions occur one after the other, branches or no branches. Secondly, this serial model enables a very large number of constrictions (here, 187) to be within the field of view of the microscope objective. A constant pressure difference when using a pressure pump, or flowrate when using a syringe pump, is maintained between the inlet and the outlet, modeled on physiological pressure gradients experienced *in vivo*, is used to advect cells through the device, one cell at a time. The minimum gaps at the constrictions (5 μm or 7 μm) are smaller than the diameter of cells but match the size of the pulmonary capillary segments, ensuring that each cell is deformed sequentially during the advection (Figure 1, top insets).

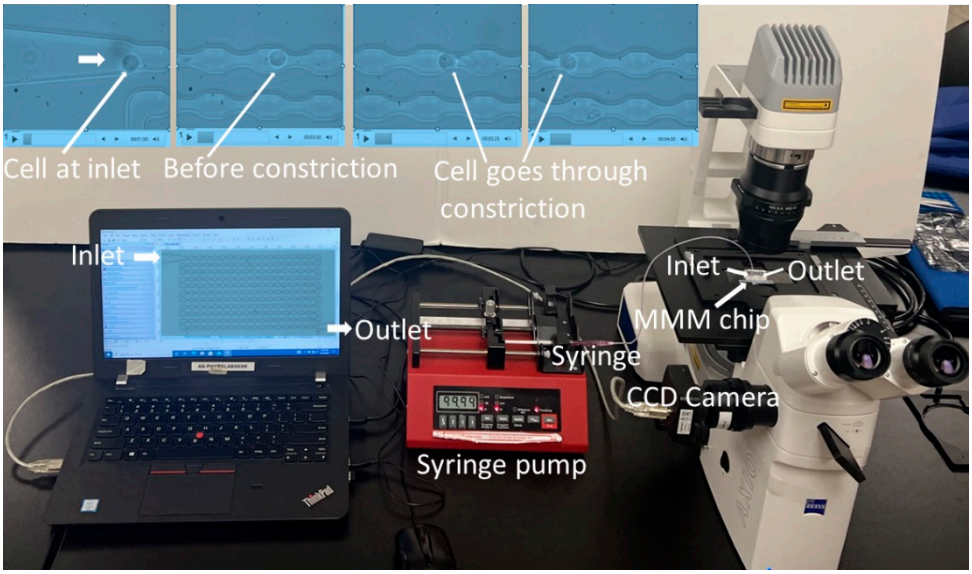

Figure 1. The microfluidic microcirculation mimetic (MMM). A picture of the entire MMM device in operation. A suspension of cells diluted in PBS or culture medium in a **syringe** is fixed to a **syringe pump,** connected by tubing to the PDMS-based MMM chip **inlet** and placed on a phase contrast/fluorescence microscope with an inverted objective lens and equipped with a **CCD camera**. The camera is connected to a **computer** which enables the running and monitoring of the device, data collection and analysis. Four screengrabs from the video (top pictures from left) show a cell at the

Preprints (www.preprints.org) | NOT PEER-REVIEWED | Posted: 4 July 2023 doi:10.20944/preprints202307.0171.v1

inlet, then before a constriction, into and out of a constriction, enabling the assessment of its deformability or mechanical properties, via its transit time through the device.

The MMM has been used for other research findings including the unravelling of some of the functions of myosin II[37]. It was the main tool used in one of the first explorations of chemotherapy-induced prometastatic changes in blood cancer cells[12]. Other clinically relevant research done using MMM (at least partially) includes the discovery that microgravity modulates effects of chemotherapeutic drugs on cancer cell migration[43]. Clinically, the MMM has been used for the *ex vivo* visualization of vaso-occlusive crises in sickle cell disease[38]. In summary, the biophysical properties of the following cell types in health and diseases have been measured using the MMM: neutrophils[35,39], leukemia cells[12], mesenchymal stromal cells[36] and red blood cells.

The MMM enables rapid measurement of hundreds of cells in less than 10 minutes, while watching in real time the fate of those cells during the advection, a step in metastasis, as would occur for circulating tumor cells (CTCs)[44,45]. Of note, it is metastasis, a complex multistep process that leads to death in over 90% of cancer cases[26,31]. Thus, MMM mimics the hematogenic microcirculation in terms of attributes such as the presence of tens to hundreds of constrictions as found in microcapillary beds *in vivo*. Furthermore, to mimic the pluronan-rich surface of the vascular endothelium, Pluronic F-127 acid (final concentration 0.1%) was added to the cell suspension before the experiments[46]. Figure 1 illustrates the procedures for running the MMM: a suspension of cells in a syringe is placed on a programmable double channel microfluidics syringe pump, NE-4002X (MA, USA), connected by tubing to the polydimethylsiloxane-based MMM chip and placed on an inverted phase contrast microscope equipped with a CCD camera. The camera is connected to a computer which enables the monitoring and running of the device, data collection and analysis. We used the MMM for the determination of transit times which is a readout of cell deformability[12,35].

2.2. Cell Culture

The K562 cells, human bone marrow derived chronic myelogenous leukemia (CML) were purchased from ATCC (K-562 ATCC ® CCL-243™) and grown in suspension using standard methods and media, namely, RPMI 1640, supplemented with 10% fetal bovine serum (FBS) and 1% Penicillin/Streptomycin. The cells were cultured in an incubator kept at 95% air; 5% CO_2 and a temperature of 37°C. We determined cell density using two methods: counting using a hemocytometer and using an automated cell counter (Invitrogen™ Countess™ II). Cell viability was also determined in two ways: Trypan blue exclusion tests and fluorescence staining with Calcein (Calcein AM, Invitrogen, C1430). The cell density for all MMM experiments was maintained at about 1 x 10^6 cells/ml, to ensure that one cell went through the device before the next arrives at the inlet, in general. Only cells at the logarithmic growth phase when viability was consistently over 96%, were used for experiments.

2.3. Drug Treatments

Chemotherapeutic interventions were done using common anti-tumor drugs, namely, nocodazole, hydroxyurea, doxorubicin and daunorubicin. Nocodazole is a cytoskeleton-changing drug and an antineoplastic agent which arrests cells in G2 or M phase. It reversibly alters dynamic instability in microtubules[29]. Hydroxyurea is an antitumor and antileukemic agent (precisely CML) which functions by inhibiting mitosis thereby blocking cell growth[47]. Doxorubicin, one of the most potent chemotherapeutic drugs, and daunorubicin, are anthracyclines which damage DNA in cancer cells and are used as first line induction therapies against leukemias and many other cancers[48]. Cytochalasin D was used to disrupt the actin cytoskeleton of cells[11,41] in view of further exploration of the cellular architectures involved in deformability measurements via transit times through the MMM. All drugs were added to the cell culture medium for MMM experiments, and the cells were incubated for 10 minutes before starting MMM experiments which were then completed at most 2 hours after the drug treatment. Hence, no cell had the drug for more than 2 hours in any MMM experiment reported here. This ensured that we were probing initial and potentially prometastatic

Preprints (www.preprints.org) | NOT PEER-REVIEWED | Posted: 4 July 2023 doi:10.20944/preprints202307.0171.v1

effects of the drugs prior to cell-killing or other cytotoxic effects. Nocodazole was used at a 5 μM final concentration[49] while hydroxyurea was used at a 100 μM final concentration. The final concentration of doxorubicin was 5 μM[12,48] while that of daunorubicin was 1 μM[12,50]. Cytochalasin D was used at a final concentration of 2 μM[11,41].

2.4. Fluorometric Morphometry

Although morphometry has been done on cells inside the MMM where shape parameters such as circularity and roundness were used to parametrize sickling of red blood cells in sickle cell disease patients[38], and although fluorescently labeled neutrophils inside the MMM have been characterized morphometrically[35], we focused on just transit times of cells through MMM in this work. However, fluorescence-guided morphometry independent of the MMM was performed using a Zeiss Vert.A1 AXIO fluorescence microscope, equipped with red, green and blue filters and with an inserted USB microscope camera (AmScope MU300), along with its AmScope (86x) image capture program. Details of the advanced fluorometric morphometry performed which yielded information on cytoplasmic cross section and nuclear cross section, following chemotherapeutic interventions, can be found in our recent publications[51,52]. Briefly, the fluorescent dyes, Hoechst 33342 (ThermoFisher Scientific), at a 0.1 mM final concentration, and Calcein AM (Invitrogen by ThermoFisher Scientific), at a final concentration of 1 μg/mL, were used to stain the nucleus and the cytoplasm, respectively, for imaging. ImageJ was used to extract cell shape and size, as well as nuclear shape and size, from the images. These morphometric measurements (size and shape), independent of MMM, serve to check whether differences in transit times are due to mechanical properties and not changes in cell size, shape or even adhesive properties.

2.5. Statistical Analysis

Analysis of variance, ANOVA, is a well-established statistical technique to analyze variations in continuous random variables measured under conditions defined by discrete factors[53] (parameters), thereby enabling the determination of the statistical significance of differences found in measured parameters. We performed statistical and error analyses using One-Way ANOVA in Origin (OriginLab, Northampton, MA, USA). We chose One-Way ANOVA or One-Way Fixed-Effects ANOVA because it is an extension of the Student 2-independent-samples *t* test and therefore enables one to simultaneously compare means among several independent samples[53]. Moreover, Origin's ANOVA algorithm minimizes the probability of type-I error in statistical analysis, where the null hypothesis is wrongly rejected, leading to the wrong conclusion that results are statistically significant. For means comparison tests in Origin's One-Way ANOVA, we selected the Tukey, Bonferroni, Dunn-Sidak and Fisher LSD, taking only those significant differences where all four tests were in agreement.

We performed error analysis using the standard error of the mean (SEM). For experiments where we expected to draw scientific conclusions, we carried out at least three independent repeats of every experiment (N1, N2 and N3). For exploratory experiments to show MMM capabilities, one experiment was done with sufficient cell numbers. In all experiments, information on cell numbers involved is provided.

3. Results

3.1. Nocodazole increases cell transit time

We used the MMM as described in the Methods section, to investigate whether nocodazole alters the mechanical properties of K562 cells in ways that might promote metastasis before cell death. Figure 2 shows that nocodazole treatment increases the transit times of cells in MMM. Figure 2(a), shows a 10% increase in mean transit time from 0.203 ∓ 0.004 s to 0.222 ∓ 0.004 s between K562 cells and K562 cells treated for 2 hours or less, with 5 μM nocodazole (K562+Noco). The box plot from one-way ANOVA shows that this increase in transit time is statistically significant (*** $p < 0.001$)). Figure 2(b) and Figure 2(c) are N2 and N3 repeats of the N1 experiment in Figure 2(a). All three repeats lead

Preprints (www.preprints.org) | NOT PEER-REVIEWED | Posted: 4 July 2023 doi:10.20944/preprints202307.0171.v1

to the same result, that nocodazole treatment increases mean cell transit times, which implies that nocodazole stiffens cells in the first 2 hours of treatment. Since chemotherapy treated cells *in vivo* include cells in the circulatory system, such stiffening or reduced deformability might increase the potential for cells to get stuck in the constrictions of the pulmonary vasculature, engendering an increased chance of extravasation and thus, increased metastatic potential.

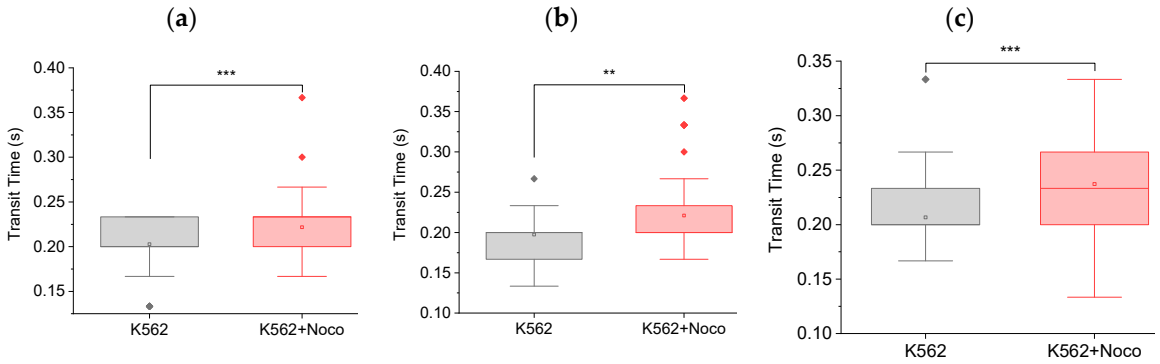

Figure 2. Nocodazole treatment increases cell transit times in MMM. Box plots from one-way ANOVA showing transit times of K562 cells and K562 cells treated for 2 hours or less, with 5 μM nocodazole (K562+Noco). The 7 μm MMM device was used. Camera framerate: 30 fps. Pump flowrate: 99.9 μl/hr. This stiffening with nocodazole was consistent in all 3 repeats: N1, N2 and N3, shown in **(a)**, **(b)** and **(c)** respectively. **(a)** N1 experiment with K562+Noco (n = 60 cells) showing a significantly higher (*** $p < 0.001$) mean transit time than untreated K562 cells (n = 60). **(b)** N2 experiment with K562+Noco (n = 60 cells) showing a significantly higher (** $p < 0.01$) mean transit time than untreated K562 cells (n = 52). **(c)**. N3 experiment with K562+Noco (n = 60 cells) showing a significantly higher (*** $p < 0.001$) mean transit time than untreated K562 cells (n = 60).

3.2. *Feasibility of Exploring Biophyical Mechanisms*

3.2.1. Feasibility Testing using Hydroxyurea

Chemotherapeutic drugs have a wide variety of molecular mechanisms by which they act on various parts of the cell to produce cytotoxic effect. Aware of the differences in the mechanisms of action of nocodazole compared to hydroxyurea (for instance, they arrest cells in slightly different phases of the cell cycle[54]), we went on to explore the feasibility of deploying the MMM to pick up such differences in view of their potentially varied contributions to chemotherapy-induced metastasis. Remarkably, as shown in Figure 3, the mean transit time of K562 cells treated with hydroxyurea was significantly (**** $p < 0.0001$) lower than that of untreated K562 cells. Note that we used the more sensitive 5 μm MMM device here (and not the 7 μm MMM of Figure 2) so that its smaller constriction size might induce more mechanical stress on cells, to produce more strain for picking up subtle mechanical differences. Figure 3 shows a 36% decrease in mean transit time, from 0.486 ∓ 0.018 s to 0.310 ∓ 0.003 s between K562 cells and K562 cells treated with hydroxyurea, respectively. This result suggests that hydroxyurea treatment may increase cell deformability in the first two hours of treatment. This indicates the feasibility of deploying the MMM to explore various biophysical readouts that may correlate or even reveal mechanisms implicated in chemotherapy-induced metastasis.

Preprints (www.preprints.org) | NOT PEER-REVIEWED | Posted: 4 July 2023 doi:10.20944/preprints202307.0171.v1

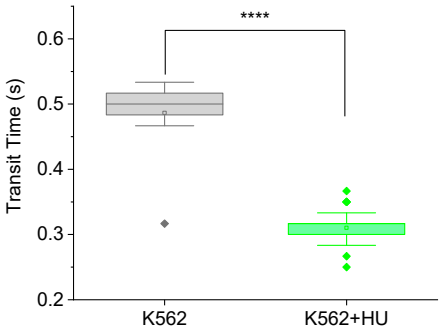

Figure 3. Feasibility of testing with hydroxyurea. Box plots showing transit times of K562 (n = 11) and K562 treated with hydroxyurea (K652 + HU, n = 60), through MMM. The 5 μm MMM device was used. Pump flowrate: 99.9 ul/hr. Camera framerate: 30 fps). The mean transit time of K562+HU is significantly (**** $p < 0.0001$) lower than K562 cells.

3.2.2. Size Effects: Independent Morphometry Tests

In our earlier work reporting how doxorubicin and daunorubicin alter cell mechanical properties in prometastatic ways[12] we monitored the morphology of cells at the time of drug treatment (0 hour), and then 2, 4, 6 and 12 hours after. It was only after 6 hours with the drugs that cell sizes showed significant changes, consistent with known cytotoxic effects. Hence, in this work, we used fluorescence-guided morphometry to check effect on cell size, 12 hours post hydroxyurea (HU) treatment. Figure 4(a) displays frequency histograms showing normally distributed cytoplasmic size of the cells. There is a shift in the distribution towards larger sizes for K562 treated with hydroxyurea. Figure 4(b) displays box plots comparing the cells in (a), showing a significant ($p < 0.001$) increase in size of cytoplasm. This result confirms that hydroxyurea treatment has some impact on the cytoplasm of cells 12 hours post. Interestingly, the trend towards increasing cell size with drug treatment makes the reduced transit time of Figure 3 even more remarkable.

Furthermore, using the same fluorescence-guided morphometry as in done for Figure 4, we extracted nuclear sizes from the cells in the experiment of Figure 4. The nuclear size results are presented in Figure 5 with frequency histograms showing normally distributed nuclear size (Figure (5a)). There is a shift in the distribution towards smaller sizes for the hydroxyurea treated cells. Figure 5(b) shows box plots comparing the cells in (a). Clearly, there is a significant ($p < 0.001$) decrease in size of nuclei due to hydroxyurea treatment.

Overall, changes in cell deformability, revealed by the MMM experiments and alterations in cytoplasmic and nuclear sizes shown via fluorescence-guided morphometry, are among biophysical properties modified by chemotherapeutic drugs. These properties can have impact on cell migration, extravasation, intravasation and advection during circulation, all of which are important steps within the metastatic cascade.

Preprints (www.preprints.org) | NOT PEER-REVIEWED | Posted: 4 July 2023 doi:10.20944/preprints202307.0171.v1

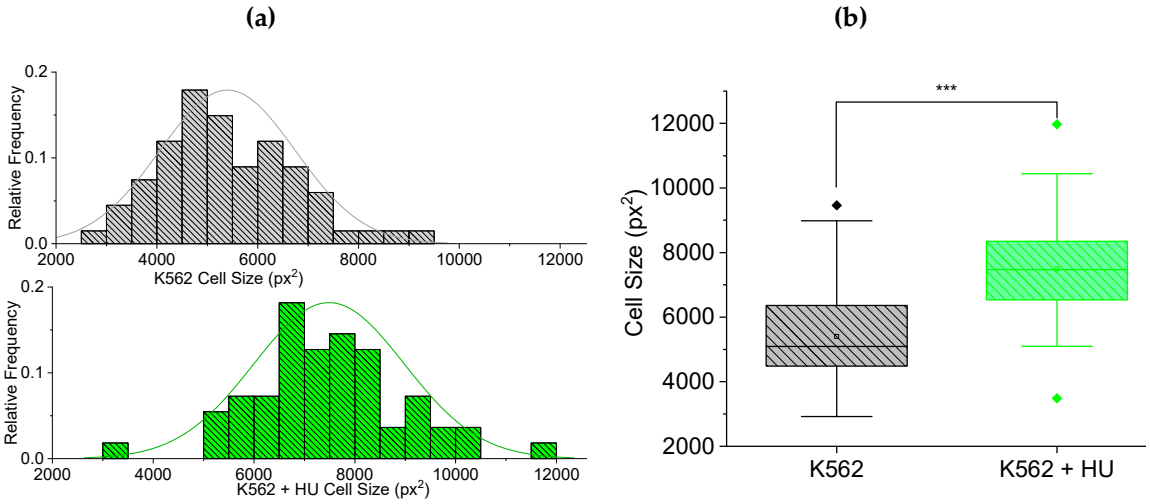

Figure 4. Fluorescence-guided morphometry to check effect on cell size, 12 hours post hydroxyurea (HU) treatment. (a) Frequency histogram showing normally distributed cytoplasmic size (cell size) of K562 (n = 67) cells and a shift in the distribution towards larger sizes for K562+HU (n = 55). **(b)** Box plots comparing the cells in (a), showing a significant ($p < 0.001$) increase in size of cytoplasm, suggesting cytoskeletal effects of HU treatment.

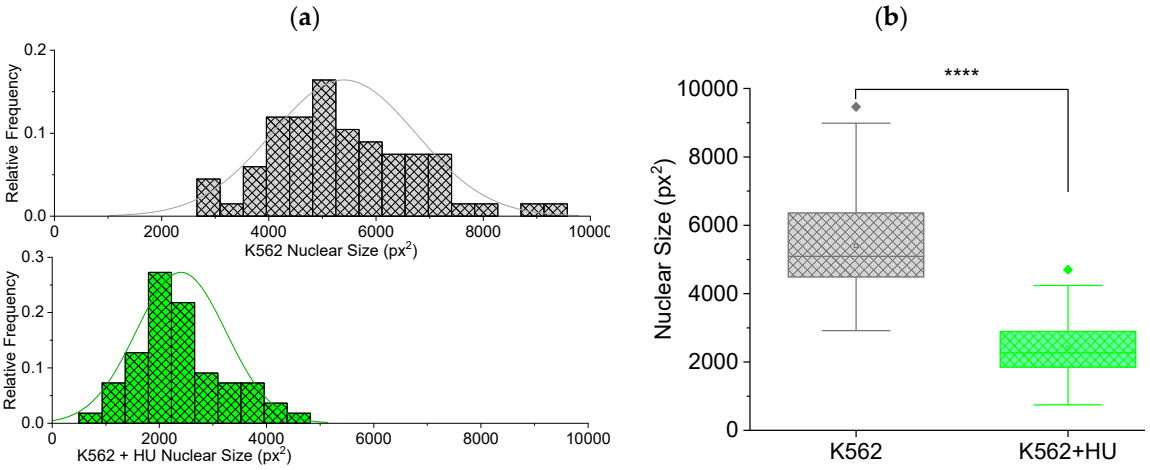

Figure 5. Fluorescence-guided morphometry to check effect on nuclear size, 12 hours post hydroxyurea (HU) treatment. (a) Frequency histogram showing normally distributed nuclear size of K562 (n = 67) cells and a shift in the distribution towards smaller sizes for K562+HU (n = 55). **(b)** Box plots comparing the cells in (a), showing a significant ($p < 0.001$) decrease in size of nuclei due to HU treatment.

3.3. Important caveat: unstable framerates can lead to inconsistent results

Obvious caveats for running microfluidic experiments accurately, or any scientific experiments, include generic verification that every equipment is functioning as expected. However, we deem it useful, as additional protocol hints, to show that fluctuating framerates which may happen when higher framerates are chosen, may lead to inconsistent results. Figure 6 shows the inconsistent results we obtained when we changed from the stable framerate of 30 fps to 60 fps, for our specific camera. The trends were inconsistent from N1 to N2 to N3. Even more convincing about the impact of framerates is Figure S1 where cytochalasin D, which disrupts F-actin and reduces the deformability of cells, showed inconsistent results due to fluctuations in framerates of 60 fps for our specific camera.

Preprints (www.preprints.org) | NOT PEER-REVIEWED | Posted: 4 July 2023 doi:10.20944/preprints202307.0171.v1

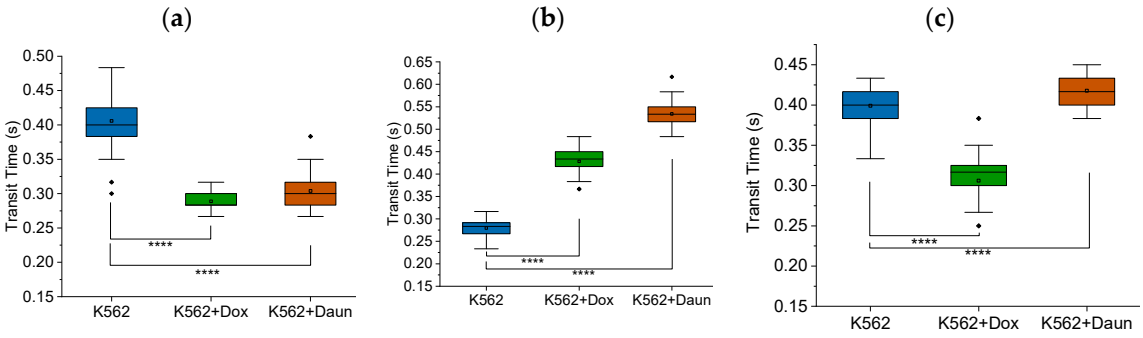

Figure 6. Unstable framerates lead to inconsistent results. Box charts from one-way ANOVA comparing transit time of K562 cells and K562 cells treated with doxorubicin (K562+Dox) and daunorubicin (K562+Daun). The 5 μm MMM device was used. Camera framerate: 60 fps. Pump flowrate: 99.9 μl/hr. The results were inconsistent due to unstable framerate when 60 fps was used: N1, N2 and N3, shown in **(a)**, **(b)** and **(c)** respectively, have different trends. In (a), (b) and (c), K562 (n = 60 cells), K562+Dox (n = 60 cells) and K562+Daun (n = 60 cells).

4. Discussion and Conclusion

Regarding our primary result that nocodazole increases cell transit time through MMM, our interpretation that increased transit time implies increased stiffness is well supported in the literature. Using atomic force microscopy to measure cell stiffness, and using fluorescence microscopy to visualize actin and microtubules, Grady et al. found that nocodazole treated cancer cells exhibited increased stiffness[55]. Matching with our experimental conditions, Ito et al. found that nocodazole treatment for 60 minutes, at a 10 μM final concentration rapidly stiffens cells[56]. Future experiments will be needed to illustrate the impact of nocodazole-induced stiffening of cancer cells on metastasis, along the lines of similar connections we found between doxorubicin induced increase in transit time through MMM and increased migration of HL60 cells via transwell migration assay[12]. Not all stiffening in MMM should be taken as implying increased migration, just as we found in the case of daunorubicin where there was increased transit time in MMM but reduced migration through pores in the transwell migration assay[12]. Different drugs and different cancer cells can be expected to show varied biophysical readouts that indicate complex mechanisms of chemotherapy-induced metastasis, just as metastasis itself has complicated and incompletely understood mechanisms. Our feasibility test with hydroxyurea illustrates this complexity. Recent work is cognizant of this complexity. For instance, Ly et al. recently measured the deformability (via transit times through microfluidic constrictions) of B-cells that survive chemotherapy, taken from acute lymphoblastic leukemia (ALL) patients treated for 7 days with a standard multidrug chemotherapy regimen of vincristine, dexamethasone, and L-asparaginase. They found that such B-cells are more deformable and distinguishable from controls (no chemo)[57]. They postulated, just as we do here, that cell physical phenotyping is a complementary prognostic tool that could guide treatment strategies and therapeutic interventions. Already, the mechanisms of chemotherapy-induced metastasis so far uncovered and the new therapeutic strategies suggest the importance of biophysical aspects[21–25].

Furthermore, our results in this work and the aforementioned corroborations in the literature illustrate general connections between chemotherapy, cell mechanics and metastasis. Some aspects of these connections have been previously reported in the scientific literature. In fact, following recent realization that key stages in the metastatic cascade such as migration, extravasation and intravasation involve the mechanical and physical properties of cells[26], physical oncology or physics of cancer[10,26,58] has emerged, clearly illustrating the connection between cell mechanics and metastasis. Although chemotherapy drugs target and kill malignant cells during cancer treatment, there is emerging evidence that such drugs inadvertently promote metastasis[5,7,8]. The reported mechanisms of chemotherapy-induced metastasis[14–19] all involve migration, extravasation, intravasation which are orchestrated by the actin-myosin cytoskeleton[11], the same determinant of cell mechanical properties, clearly indicating the connection between cell mechanics and chemotherapy-induced metastasis.

Preprints (www.preprints.org) | NOT PEER-REVIEWED | Posted: 4 July 2023 doi:10.20944/preprints202307.0171.v1

Furthermore, in spite of the very wide variety of cancers with respect to their molecular biology, pathogenesis and prognosis[59], metastasis occurs in all cancers, as we noted already. Thus, there is an urgent need for anti-metastasis therapy[6], against all metastatic cancers, and not only against the chemotherapy-induced metastasis. Incidentally, cellular mechanical properties have been shown to be good markers for metastatic potential of cancer cells[60,61] and can be used for diagnosis of cancer itself[9,34,62]. Hence, this work which explores the role of cell mechanics in chemotherapy-induced metastasis also addresses the role of cell mechanics in metastasis in general. Finally, it makes the case that cell mechanical properties should become therapeutic targets against both chemotherapy-induced metastasis as well as metastasis in general. This could lead to better treatment outcomes against cancers.

Supplementary Materials: The following supporting information can be downloaded at: www.mdpi.com/xxx/s1, Figure S1: **Important caveats for running the MMM**.

Author Contributions: Conceptualization, A.E.; methodology, A.E.,S.V.,C.N.,M.J.,G.K. and D.J; software, A.A., S.V., N.H.,I.B.,M.M.; validation, A.E.,A.A., S.V., N.H.,I.B., and M.M.; formal analysis, A.A.,S.V.,N.H.,I.B., and M.M.; investigation, A.A.,S.V.,N.H.,I.B.,C.N.,M.J.,G.K.,D.J.,M.M.,S.M.,A.T., and C.P.; resources, A.E.; data curation, A.E.; writing—original draft preparation, A.E., A.A.,S.V.; writing—review and editing, A.E.; visualization, A.E.,A.A.,S.V.,N.H.,I.B., and M.M.; supervision, A.E.; project administration, A.E.; funding acquisition, A.E., C.N., and S.V. All authors have read and agreed to the published version of the manuscript.

Funding: This research received no external funding. This work received funding support from the Creighton University Startup Grant 240133 (to AE), the Creighton University Center for Undergraduate Research (CURAS) SURF (VS) and Creighton's Clare Boothe Luce Award (to CN).

Data Availability Statement: Data is contained within the article and within supplementary material.

Acknowledgments: Authors acknowledge the collegiality and support of other members of the Translational Biomedical Physics (TBP) research group and the entire Physics Department where the TBP Lab is located.

Conflicts of Interest: The authors declare no conflict of interest.

References

1. Mehlen, P. & Puisieux, A. Metastasis: a question of life or death. *Nat. Rev. Cancer* **6**, 449–458 (2006).
2. Seyfried, T. N. & Huysentruyt, L. C. On the origin of cancer metastasis. *Crit. Rev. Oncog.* **18**, 43–73 (2013).
3. Steeg, P. S. Tumor metastasis: mechanistic insights and clinical challenges. *Nat. Med.* **12**, 895–904 (2006).
4. Fouad, Y. A. & Aanei, C. Revisiting the hallmarks of cancer. *Am. J. Cancer Res.* **7**, 1016–1036 (2017).
5. Ran, S. The role of TLR4 in chemotherapy-driven metastasis. *Cancer Res.* **75**, 2405–2410 (2015).
6. Weber, G. F. Why does cancer therapy lack effective anti-metastasis drugs? *Cancer Lett.* **328**, 207–11 (2013).
7. Volk-Draper, L. *et al.* Paclitaxel therapy promotes breast cancer metastasis in a TLR4-dependent manner. *Cancer Res.* **74**, 5421–34 (2014).
8. Geldof, A. A. & Rao, B. R. Doxorubicin treatment increases metastasis of prostate tumor (R3327-MatLyLu). *Anticancer Res.* **8**, 1335–9 (1988).
9. Suresh, S. Biomechanics and biophysics of cancer cells. *Acta Biomater.* **3**, 413–438 (2007).
10. Moore, N. M. & Nagahara, L. A. Physical biology in cancer. 1. Cellular physics of cancer metastasis. *Am. J. Physiol. Cell Physiol.* **306**, C78-9 (2014).
11. Man, S. M. *et al.* Actin polymerization as a key innate immune effector mechanism to control Salmonella infection. *Proc. Natl. Acad. Sci. U. S. A.* **111**, (2014).
12. Prathivadhi-Bhayankaram, S. V. *et al.* Chemotherapy impedes in vitro microcirculation and promotes migration of leukemic cells with impact on metastasis. *Biochem. Biophys. Res. Commun.* **479**, 841–846 (2016).
13. Lam, W. A., Rosenbluth, M. J. & Fletcher, D. A. Chemotherapy exposure increases leukemia cell stiffness. *Blood* **109**, 3505–8 (2007).
14. Karagiannis, G. S. *et al.* Neoadjuvant chemotherapy induces breast cancer metastasis through a TMEM-mediated mechanism. *Sci. Transl. Med.* **9**, (2017).
15. D'Alterio, C., Scala, S., Sozzi, G., Roz, L. & Bertolini, G. Paradoxical effects of chemotherapy on tumor relapse and metastasis promotion. *Seminars in Cancer Biology* **60**, 351–361 (2020).
16. Karagiannis, G. S., Condeelis, J. S. & Oktay, M. H. Chemotherapy-Induced Metastasis: Molecular Mechanisms, Clinical Manifestations, Therapeutic Interventions. (2019). doi:10.1158/0008-5472.CAN-19-1147

Preprints (www.preprints.org) | NOT PEER-REVIEWED | Posted: 4 July 2023 doi:10.20944/preprints202307.0171.v1

17. Ortiz-Otero, N., Marshall, J. R., Lash, B. & King, M. R. Chemotherapy-induced release of circulating-tumor cells into the bloodstream in collective migration units with cancer-associated fibroblasts in metastatic cancer patients. *BMC Cancer* **20**, 873 (2020).
18. Bellomo, G. *et al.* Chemotherapy-induced infiltration of neutrophils promotes pancreatic cancer metastasis via Gas6/AXL signalling axis. *Gut* **0**, gutjnl-2021-325272 (2022).
19. Mansouri, N. *et al.* Role of extracellular vesicles in chemotherapy-induced lung metastasis. in *European Respiratory Journal* **56**, 3944 (European Respiratory Society (ERS), 2020).
20. Zarfati, A. *et al.* Chemotherapy-induced cavitating Wilms' tumor pulmonary metastasis: Active disease or scarring? A case report and literature review. *Front. Pediatr.* **11**, (2023).
21. Monteran, L. *et al.* Chemotherapy-induced complement signaling modulates immunosuppression and metastatic relapse in breast cancer. *Nat. Commun.* **13**, (2022).
22. Su, J. xuan *et al.* Chemotherapy-induced metastasis: molecular mechanisms and clinical therapies. *Acta Pharmacologica Sinica* (2023). doi:10.1038/s41401-023-01093-8
23. Li, Q. *et al.* Chemotherapy-Induced Senescence Reprogramming Promotes Nasopharyngeal Carcinoma Metastasis by circRNA-Mediated PKR Activation. *Adv. Sci.* **10**, (2023).
24. Zhu, C. *et al.* Near-Death Cells Cause Chemotherapy-Induced Metastasis via ATF4-Mediated NF-κB Signaling Activation. *Adv. Sci.* **10**, (2023).
25. Li, T. *et al.* Therapeutic Nanocarriers Inhibit Chemotherapy-Induced Breast Cancer Metastasis. *Adv. Sci.* **9**, (2022).
26. Wirtz, D., Konstantopoulos, K. & Searson, P. C. The physics of cancer: the role of physical interactions and mechanical forces in metastasis. *Nat. Rev. Cancer* **11**, 512–22 (2011).
27. Gensbittel, V. *et al.* Mechanical Adaptability of Tumor Cells in Metastasis. *Developmental Cell* **56**, 164–179 (2021).
28. Mierke, C. T. Mechanical Cues Affect Migration and Invasion of Cells From Three Different Directions. *Frontiers in Cell and Developmental Biology* **8**, 946 (2020).
29. Vasquez, R. J., Howell, B., Yvon, A. M. C., Wadsworth, P. & Cassimeris, L. Nanomolar concentrations of nocodazole alter microtubule dynamic instability in vivo and in vitro. *Mol. Biol. Cell* **8**, 973–985 (1997).
30. Hanahan, D. & Weinberg, R. A. The hallmarks of cancer. *Cell* **100**, 57–70 (2000).
31. Liu, Y.-N., Kang, B.-B. & Chen, J. H. Transcriptional regulation of human osteopontin promoter by C/EBPalpha and AML-1 in metastatic cancer cells. *Oncogene* **23**, 278–88 (2004).
32. Wu, P.-H. *et al.* A comparison of methods to assess cell mechanical properties. *Nat. Methods* (2018). doi:10.1038/s41592-018-0015-1
33. Otto, O. *et al.* Real-time deformability cytometry: on-the-fly cell mechanical phenotyping. *Nat. Methods* **12**, 199–202 (2015).
34. Tse, H. T. K. *et al.* Quantitative diagnosis of malignant pleural effusions by single-cell mechanophenotyping. *Sci. Transl. Med.* **5**, 212ra163 (2013).
35. Ekpenyong, A. E. *et al.* Mechanical deformation induces depolarization of neutrophils. *Sci. Adv.* **3**, (2017).
36. Tietze, S. *et al.* Spheroid Culture of Mesenchymal Stromal Cells Results in Morphorheological Properties Appropriate for Improved Microcirculation. *Adv. Sci.* **6**, 1802104 (2019).
37. Chan, C. J. *et al.* Myosin II Activity Softens Cells in Suspension. *Biophys. J.* **108**, 1856–69 (2015).
38. Asuquo, M. I. *et al.* Microfluidic Microcirculation Mimetic as a Tool for the Study of Rheological Characteristics of Red Blood Cells in Patients with Sickle Cell Anemia. *Appl. Sci.* **12**, 4394 (2022).
39. Ekpenyong, A. E., Toepfner, N., Chilvers, E. R. & Guck, J. Mechanotransduction in neutrophil activation and deactivation. *Biochim. Biophys. Acta - Mol. Cell Res.* **1853**, 3105–3116 (2015).
40. Guck, J. *et al.* The optical stretcher: a novel laser tool to micromanipulate cells. *Biophys. J.* **81**, 767–84 (2001).
41. Ekpenyong, A. E. *et al.* Viscoelastic Properties of Differentiating Blood Cells Are Fate- and Function-Dependent. *PLoS One* **7**, e45237 (2012).
42. Rowat, A. C. *et al.* Nuclear envelope composition determines the ability of neutrophil-type cells to passage through micron-scale constrictions. *J. Biol. Chem.* **288**, 8610–8 (2013).
43. Prasanth, D. *et al.* Microgravity Modulates Effects of Chemotherapeutic Drugs on Cancer Cell Migration. *Life* **10**, 162 (2020).
44. Chaffer, C. & Weinberg, R. A Perspective on Cancer Cell Metastasis. *Science (80-.).* **331**, 1559–1565 (2011).
45. Koumoutsakos, P., Pivkin, I. & Milde, F. The Fluid Mechanics of Cancer and Its Therapy. *Annu. Rev. Fluid Mech.* **45**, 325–355 (2013).
46. Luk, V. N., Mo, G. C. & Wheeler, A. R. Pluronic additives: a solution to sticky problems in digital microfluidics. *Langmuir* **24**, 6382–9 (2008).
47. Madaan, K., Kaushik, D. & VerM.A., T. Hydroxyurea: A key player in cancer chemotherapy. *Expert Rev. Anticancer Ther.* **12**, 19–29 (2012).
48. Douedi, S. & Carson, M. P. *Anthracycline Medications (Doxorubicin). StatPearls* (StatPearls Publishing, 2020).
49. Hamm-Alvarez, S. F., Sonee, M., Loran-Goss, K. & Shen, W. C. Paclitaxel and nocodazole differentially alter endocytosis in cultured cells. *Pharm. Res.* **13**, 1647–1656 (1996).

Preprints (www.preprints.org) | NOT PEER-REVIEWED | Posted: 4 July 2023 doi:10.20944/preprints202307.0171.v1

50. Wojcik, T. *et al.* Comparative endothelial profiling of doxorubicin and daunorubicin in cultured endothelial cells. *Toxicol. In Vitro* **29**, 512–21 (2015).
51. Walter, Y. *et al.* Development of In Vitro Assays for Advancing Radioimmunotherapy against Brain Tumors. *Biomedicines* **10**, 1796 (2022).
52. McKinley, S. *et al.* Microgravity-Induced Changes to Drug Response in Cancer Cells Quantified Using Fluorescence Morphometry. (2023). doi:10.20944/PREPRINTS202306.1494.V1
53. Larson, M. G. Analysis of variance. *Circulation* **117**, 115–121 (2008).
54. Apraiz, A., Mitxelena, J. & Zubiaga, A. Studying cell cycle-regulated gene expression by two complementary cell synchronization protocols. *J. Vis. Exp.* **2017**, 55745 (2017).
55. Grady, M. E., Composto, R. J. & Eckmann, D. M. Cell elasticity with altered cytoskeletal architectures across multiple cell types. *J. Mech. Behav. Biomed. Mater.* **61**, 197–207 (2016).
56. Ito, S. *et al.* Induced cortical tension restores functional junctions in adhesion-defective carcinoma cells. *Nat. Commun.* **8**, (2017).
57. Ly, C. *et al.* Altered physical phenotypes of leukemia cells that survive chemotherapy treatment. *Integr. Biol. (Camb).* **15**, (2023).
58. Munbodh, R. & Jackson, A. Quantifying cell migration distance as a contributing factor to the development of rectal toxicity after prostate radiotherapy. *Med. Phys.* **41**, 021724 (2014).
59. Fritsch, A. *et al.* Are biomechanical changes necessary for tumour progression? *Nat. Phys* **6**, 730–732 (2010).
60. Swaminathan, V. *et al.* Mechanical stiffness grades metastatic potential in patient tumor cells and in cancer cell lines. *Cancer Res.* **71**, 5075–80 (2011).
61. Guck, J. *et al.* Optical deformability as an inherent cell marker for testing malignant transformation and metastatic competence. *Biophys. J.* **88**, 3689–98 (2005).
62. Remmerbach, T. W. *et al.* Oral cancer diagnosis by mechanical phenotyping. *Cancer Res.* **69**, 1728–32 (2009).
63. Lee, B. H., Suresh, S. & Ekpenyong, A. Fluorescence intensity modulation of CdSe/ZnS quantum dots assesses ROS during chemotherapy and radiotherapy for cancer cells. *J. Biophotonics* **12**, e201800172 (2018).
64. Djam, K. H., Lee, B. H., Suresh, S. & Ekpenyong, A. E. Quantum Dots for Assessment of Reactive Oxygen Species Accumulation During Chemotherapy and Radiotherapy. in *Methods in Molecular Biology* **2135**, 293–303 (Humana Press Inc., 2020).
65. Gossett, D. R. *et al.* Hydrodynamic stretching of single cells for large population mechanical phenotyping. *Proc Natl Acad Sci USA* **109**, 7630–7635 (2012).

Disclaimer/Publisher's Note: The statements, opinions and data contained in all publications are solely those of the individual author(s) and contributor(s) and not of MDPI and/or the editor(s). MDPI and/or the editor(s) disclaim responsibility for any injury to people or property resulting from any ideas, methods, instructions or products referred to in the content.